AD-A070 890   NAVAL RESEARCH LAB WASHINGTON DC   F/G 20/9

GENERATION OF A ROTATING LIQUID LINER BY TANGENTIAL INJECTION. (U)

JUN 79 R L BURTON, P J TURCHI, D J JENKINS

UNCLASSIFIED   NRL-MR-4025   NL

| OF |

AD
A070890

END
DATE
FILMED
8-79
DDC

NRL Memorandum Report 4025

Generation of a Rotating Liquid Liner by Tangential Injection

R. L. Burton, P. J. Turchi, D. J. Jenkins,
R. E. Lanham, J. Cameron, and A. L. Cooper

Plasma Physics Division

June 25, 1979

NAVAL RESEARCH LABORATORY
Washington, D.C.

SECURITY CLASSIFICATION OF THIS PAGE (When Data Entered)

REPORT DOCUMENTATION PAGE		READ INSTRUCTIONS BEFORE COMPLETING FORM
1. REPORT NUMBER NRL Memorandum Report 4025	2. GOVT ACCESSION NO.	3. RECIPIENT'S CATALOG NUMBER
4. TITLE (and Subtitle) (6) GENERATION OF A ROTATING LIQUID LINER BY TANGENTIAL INJECTION,		5. ~~TYPE OF REPORT~~ & PERIOD COVERED (9) Interim report on a continuing ~~NRL problem~~
		6. PERFORMING ORG. REPORT NUMBER
7. AUTHOR(s) (10) R. L. Burton*, P. J. Turchi, D. J. Jenkins, R. E. Lanham, J. Cameron* ~~and A. L. Cooper~~		8. CONTRACT OR GRANT NUMBER(s) (11) 25 Jun 79
9. PERFORMING ORGANIZATION NAME AND ADDRESS Naval Research Laboratory Washington, DC 20375 (12) 18 p.		10. PROGRAM ELEMENT, PROJECT, TASK AREA & WORK UNIT NUMBERS NRL Problem H02-28D and H02-26E RR011-09-41, 61153N-11
11. CONTROLLING OFFICE NAME AND ADDRESS Department of the Navy and Department of Energy Office of Naval Research — Washington, DC 20545 Arlington, VA 22217		12. REPORT DATE June 25, 1979
		13. NUMBER OF PAGES 17
14. MONITORING AGENCY NAME & ADDRESS (if different from Controlling Office) (14) NRL-MR-4025		15. SECURITY CLASS. (of this report) UNCLASSIFIED
		15a. DECLASSIFICATION/DOWNGRADING SCHEDULE

16. DISTRIBUTION STATEMENT (of this Report)

Approved for public release; distribution unlimited.

17. DISTRIBUTION STATEMENT (of the abstract entered in Block 20, if different from Report)

(16) RR01109 (17) RR0110941

18. SUPPLEMENTARY NOTES

For distribution to UC-20, b, c, d, e, and f.
*JAYCOR, Alexandria, VA

19. KEY WORDS (Continue on reverse side if necessary and identify by block number)

LINUS concept
Implosion chamber
Imploding liquid liners

20. ABSTRACT (Continue on reverse side if necessary and identify by block number)

Efficient compression of low mass-density payloads by the implosion of higher mass-density liquid cylinders or liners, as in the NRL LINUS concept for controlled thermonuclear fusion, requires rotation of the liner material to avoid Rayleigh-Taylor instabilities at the liner-payload interface. Experimentally, such implosions have been demonstrated with liners formed within rotating implosion chambers. The present work uses a scale-model experimental apparatus to investigate the possibility of creating liner rotation by tangential injection of the liquid liner

(Continues)

DD FORM 1 JAN 73 1473 EDITION OF 1 NOV 65 IS OBSOLETE
S/N 0102-014-6601

SECURITY CLASSIFICATION OF THIS PAGE (When Data Entered)

251 950

20. Abstract (Continued)

material. Different modes of behavior are obtained depending on the fluid exhaust procedures. Right-circular, cylindrical free surfaces are achieved with axial exhaust of fluid at radii interior to the injection nozzles, for which the liner exhibits a combination of solid-body and free vortex flows in different regions. Measurements allow estimates of power losses to viscous shear, turbulence, etc. A simple model based on open-channel flow is then derived, which is in good agreement with experiment, and is used to extrapolate results to the scale of a possible LINUS fusion reactor.

CONTENTS

GENERATION OF A ROTATING LIQUID LINER BY TANGENTIAL INJECTION

I. INTRODUCTION

Plasma heating by imploding liquid liners is being investigated, at the Naval Research Laboratory, as an attractive concept for a thermonuclear fusion reactor. In the LINUS concept (1), a stable D-T plasma is created in the cavity formed by rotating a liquid metal cylinder or liner inside a partially filled pressure vessel. A cylindrical free surface is thus formed at a radius r_{10}, surrounding a plasma and magnetic field. The liner rotation must be sufficient to prevent Rayleigh-Taylor instability of the inner free surface of the liner during final compression of the plasma and magnetic field (2,3). The liner is constrained on its outer surface by a free piston, which can be rapidly accelerated by a high pressure gas driver. The resulting free piston displacement produces an inward radial motion $r_1(t)$ of the free surface, which at high magnetic Reynolds number produces an adiabatic compression of the magnetic field and plasma, raising the plasma temperature above thermonuclear ignition. The resulting energetic neutrons are captured in the liner to raise its temperature, react with Li to breed tritium, and protect the reactor structure from radiation damage. This process in a reactor is typically repeated at a rate of a few Hz.

A number of experiments and theoretical studies of the LINUS concept have been performed (1, 3-7). In all laboratory experiments to date, the initial liner configuration has been created by rotating the entire pressure vessel (implosion chamber) ,

Note: Manuscript submitted April 19, 1979.

so that the liquid is in solid-body rotation when the implosion begins. If this approach is carried to the reactor stage, rotation of the implosion chamber implies that a number of difficult engineering problems must be addressed, such as design of support bearings and bearing lubricant, and design of a rotating vacuum seal and a high pressure seal for the piston gas drive.

Simple heat balance calculations on reactor-sized systems producing power at a level of several hundred MW(t) show that a liner volumetric flow rate of several m^3/sec is required, and that this must be supplied by external pumps, directly coupled to a set of exit turbines to recover the considerable discharge kinetic energy of the liquid metal. If these same pumps could be used to provide liner rotation, then the above mentioned engineering complications associated with a rotating implosion chamber could be avoided. A small scale experiment is described here in which a rotating liner is created by tangential injection of liquid, and measurements are made to determine the power consumed. A simple channel-flow model is invoked to explain the power loss by turbulent shear at the chamber walls, and to estimate the power consumed in a reactor application.

II. DESCRIPTION OF THE APPARATUS

In Fig. 1, a schematic is shown of the cylindrical vessel or 'swirl chamber' with tangential-injection nozzles at the outer radius and exit ports mounted in the side wall. The swirl chamber has a radius of 12.5 cm and a length of 6.8 cm. Four linear tangential-

injection nozzles are provided, each with a rectangular 0.68 cm^2 throat of dimensions 6.8 cm x 1.0 mm. The nozzles are fed from a manifold encircling the chamber through four 1.76 cm^2 hoses, which enter radially at the outer wall. The flow turns 90^o into a 6.8 cm x 3 mm settling chamber upstream of the nozzle, and then discharges along the outer wall.

A variety of exhaust ports are provided in the chamber. A 4 cm diameter port at the center exposes the free surface to atmospheric pressure at all times. Four sets of twin discharge ports of 1.33 cm^2, are located midway between the injection nozzles in the outer wall, (Fig. 1) permitting radial discharge flow. These ports connect through eight 1.5 cm diameter hoses to a valved manifold, permitting the flow rate to be controlled. Finally, a ring of 8 ports, 1.3 cm in diameter and placed at 10 cm radius, are located in one end wall of the chamber. These ports are connected through 1.5 cm diameter hoses to a common valved manifold, allowing the flow rate to be controlled.

The end wall opposite these exhaust ports is made of Plexiglas so that photographs of the swirling flow can be taken. A static pressure gauge in the outer wall reads the rotational head of the spinning fluid, and a pressure gauge on inlet manifold gives the source pressure. The rotational speed of the free surface was measured by seeding the flow with 3 mm diameter styrofoam balls which floated on the surface and were then illuminated with a variable-frequency stroboscopic light source.

III. FLOW DESCRIPTION

The initial concept was to inject fluid tangentially and extract it at the outer wall, so that the liquid flow interior to a thin layer at the outer wall would approximate solid body rotation. However, it was not possible by this method to produce a circular free surface. Instead, the inner surface of the fluid formed a twisted cylinder of quasi-elliptical cross-section whose major axis varied in orientation by 90° from one endwall to the other. This non-circular condition is remedied by allowing liquid to discharge axially through the chamber end wall, until approximately 50% is discharging radially and 50% axially. This produces a turbulent but steady free surface of circular cross section. As the percentage of axial discharge is increased and the radial discharge is correspondingly decreased, the free surface remains circular and steady. The chamber can be operated with 50 to 100% of the flow discharging axially. The case of 100% axial discharge provides the simplest flow pattern, so that the radial discharge at the outer surface was reduced to zero for the experiments.

At the maximum flow rate of 3.3 l/sec the diameter of the free surface is 14.8 cm, which is smaller than the location of the axial exhaust ports. This means that the fluid between the free surface and these axial ports should nearly be in solid body rotation. The flow pattern between the axial exhaust ports and the outer wall is more complicated, and can be divided into two regions. In the inner region, flow is rotational and possesses an inward radial velocity, similar to a free vortex. In the outer region the flow

is azimuthally periodic, having a high tangential velocity at the nozzle exit, (and zero velocity at the radial exhaust ports, if these are in use).

IV. EXPERIMENT

With a circular free surface established in the chamber, the following quantities were measured (Table I):

Table I

Total injected flow rate, Q_{INJ}:	3.3 l/sec
Supply pressure:	2.43 atm (gauge)
Outer wall static pressure, p_w	0.32 atm (gauge)
Free surface pressure, p_1:	0.00 atm (gauge)
Free surface radius, r_1:	7.4 cm
Free surface rotational speed, ω_1:	63 radians/sec

From this data the following quantities are calculated (Table II).

Table II

Nozzle throat injection velocity, V_{INJ}:	11.3 m/sec
Exhaust flow velocity, V_E:	3.5 m/sec
Free surface rotational velocity, V_{θ_1}:	4.7 m/sec
Fluid power injected, $\frac{1}{2}\dot{m}V^2_{INJ}$:	212 watts
Fluid power exhausted, $\frac{1}{2}\dot{m}V^2_E$:	20 watts

V. SWIRL CHAMBER FLOW MODEL

In order to calculate the relative importance of various power dissipation mechanisms in the swirl chamber, a velocity distribution consistent with the experiment must be estimated. The flow is assumed

to be independent of axial position, and is divided radially into three regions as discussed above. In the inner region, inside the radius, r_E, of the axial exhaust ducts, the radial velocity is zero. This flow is taken to be in solid body rotation, with the inner free surface rotating at 4.7 m/sec. For radii larger than the exhaust ports the flow divides into two regions. The injected fluid forms a radially thin jet at the outer wall, and mixes turbulently with an inner, azimuthally uniform flow which behaves as a free vortex.

The inner solid body azimuthal velocity is

$$V = V_1 r/r_1 \qquad r \le r_E$$

where V_1 is the measured azimuthal free surface velocity. Conserving angular momentum, Vr, in the free vortex flow gives

$$V = V_1 r^2_E/r_1 r \qquad r \ge r_E$$

The free vortex flow must now be matched to the injection region. This is done in a consistent manner by assuming that the jet flow from the tangential injection nozzles expands radially inward, such that the mean jet velocity equals the free vortex velocity. Thus, if the jet thickness is δr and the nozzle width is Δr, the radius $r^* = r_w - \delta r$ at which the jet and free vortex flows match is defined by:

$$V^* = V_{INJ} \left(\frac{\Delta r}{r_w - r^*}\right) = \frac{V_1 r_E^2}{r_1 r^*}$$

Solving for r^*:

$$r^* = \frac{r_w}{1 + \frac{V_{INJ}}{V_1} \frac{r_1 \Delta r}{r_E^2}}$$

and for δr:

$$\delta r = r_w - r^* = r_w \left(1 - \frac{1}{1 + \frac{V_{INJ}}{V_1} \frac{r_1 \Delta r}{r_E^2}}\right) \approx r_w \frac{V_{INJ}}{V_1} \frac{r_1 \Delta r}{r_E^2}$$

For $\Delta r = 0.1$ cm, $\delta r = 0.225$ cm, so $r^* = 12.275$ cm and $V^* = 5.17$ m/sec.

The mean velocity on the outer wall will lie between V^* and V_{INJ}. Transition from V_{INJ} to V^* will occur over a jet length estimated by assuming that the jet inner boundary is parallel to streamlines of the free vortex flow. The radial velocity U^* is

$$U^* = \frac{Q_{INJ}}{2\pi r^* h} = 6.26 \text{ cm/sec}$$

The streamline slope is $S = U^*/V^* = 0.0121$, from which the jet length is $L = (\delta r - \Delta R)/S = 10.3$ cm, corresponding to an angular transition distance of 47.4 degrees. For a linear variation of velocity during transition, the mean speed at the wall is $V(r_w) = 6.78$ m/sec. The complete radial distribution of V can be modelled as shown in Fig. 2 . The velocity distribution of Fig. 2 can then be integrated to find the azimuthal flow:

$$Q_\theta = \int hV(r)dr$$

which gives Q_θ = 19.4 l/sec.

VI. POWER LOSS CALCULATIONS

The injected fluid power (Table II) is 212 watts. This power is distributed to exhaust flow power (20 watts), pressure drop at the entrance to the exhaust duct, turbulent mixing of the jet, and turbulent shear at the wall.

The exhaust duct pressure drop is approximately equal to ρV^2_{ex} for sharp-edged entrance, giving $\Delta p_E = 0.124$ atm. The power loss is $P_E = \Delta p_E Q_{INJ} = 41$ watts. The power loss to jet mixing is $P_J = \frac{1}{2}\rho Q_{INJ}(V_{INJ} - V^*)^2 = 62$ watts. The turbulent shear at the wall is estimated by adopting an Open Channel Flow Model (9), which is used to calculate the hydraulic slope required for gravity flow of a liquid at a given speed in an open duct. The hydraulic slope is

$$S = \frac{f\bar{V}^2}{8gm}$$

where f, the Darcey-Weisbach friction coefficient, is a function of surface roughness and Reynolds number, $\bar{V}$ is the mean flow velocity in the channel, g is the acceleration of gravity and m is the hydraulic radius, defined as flow cross sectional area divided by the wetted perimeter. For this experiment m = 2.03 cm.

Because the velocity V varies considerably with radius, we use $\overline{V^2}$ instead of $\bar{V}^2$ in calculating the hydraulic slope. From the velocity

distribution (Fig. 2) we get $(\overline{V^2})^{\frac{1}{2}} = 5.63$ m/sec. The Reynolds number based on $(\overline{V^2})^{\frac{1}{2}}$ and m is Re = 11,500, which for a relative roughness of .002 gives f = .033 (9). Thus the hydraulic slope is S = .669. The equivalent pressure drop over the channel length ℓ is $\Delta p_\theta = \rho g \ell S$, where ℓ is taken as the circumference at the mean channel radius. The calculated value is $\Delta p_\theta = .0412$ atm. The power dissipated in wall shear is thus calculated to be $P_\theta = Q_\theta \Delta p_\theta = 80$ watts. The calculated power loss mechanisms are shown in Table III:

Table III

Calculated Power Losses in the Swirl Chamber

Exhaust Flow Power	20 watts
Exhaust Duct Pressure Drop	41 watts
Turbulent Jet Mixing	62 watts
Wall Shear Loss	80 watts
Calculated Loss:	203 watts
Measured P_{INJ}:	212 watts

The calculated loss accounts for the measured power input to within 4%, which must be regarded as good agreement considering the approximate character of the model used. For example, the open channel flow model underestimates the dissipation at the outer radius, where the velocity is considerably higher than the mean value of $\bar{V}$ used in the calculations.

Extrapolation to LINUS Fusion Reactors

In the case of a LINUS fusion reactor system (8), the initial

inner surface radius and tangential speed would be about one meter and 20 m/sec, respectively, using a liner of lead-lithium alloy at about 700-800^{o}K, ($\rho \approx 10^{4}$ kg/m^{3}). With fixed flow geometry (and the same relative roughness factor of 0.002), the power losses in a reactor-size system can be scaled from the present swirl chamber experiment as shown in Table IV:

Table IV

Scaled Estimates of Power Losses in LINUS Reactor

Exhaust Duct Pressure Drop	6.9 MW
Turbulent Jet Mixing	10.5 MW
Wall Shear Loss	9.4 MW
Total Loss	27 MW

For a LINUS fusion reactor scenario (as discussed in Ref. 8), with a thermonuclear energy gain relative to total energy of 1.5, and a peak operating magnetic field of 0.8 MG, a module based on a simple scale-up of the swirl chamber would provide about 216 MJ of thermal energy or about 72 MJ of electrical energy each shot. In order for the flow power losses to be less than ten percent of the electrical output of the reactor, the implosion repetition rate must exceed 3.7 Hz. The net electrical power per module would then be about 240 MW. Under these same conditions, the volume flow rate of liner material for a mean temperature excursion of 100^{o}C is 4.5 m^{3}/sec, compared to a scaled-up injection flow rate of 2.7 m^{3}/sec to provide liner rotation. Thus, power losses and turbulence levels associated with liner circulation to limit the temperature excursion of the

liner material can be comparable to those incurred in using tangential injection to create liner rotation. Separate study (10) has indicated that fluid-bearing losses involved in rotating the entire implosion chamber are comparable to those estimated for the tangential injection approach. Thus, considerable gain in simplicity of LINUS reactor operation may be possible without incurring significantly worse performance by use of tangential fluid injection to form the rotating liquid liner.

VII. CONCLUSIONS

Experimental tests with the swirl chamber demonstrate the formation of rotating liquid liners by tangential injection of fluid. Cylindrical inner surfaces with satisfactory circularity and axial uniformity are achieved with tangential injection at the outer radius of the chamber and substantial (>50%) extraction of the fluid mass flow at inner radii through ports in the sidewalls. A model of the azimuthal and radial fluid velocity distributions provides a reasonable basis for estimates of power losses in terms of an open-channel shear flow and turbulent entrance and exit conditions. The calculated power loss is in good agreement with experimental measurement lending credence to the flow model and allowing extrapolation of calculations to larger devices.

VIII. REFERENCES

1. Turchi, P.J., Book, D.L., Burton, R.L., and Cooper, A.L., "Stabilized Imploding Liner Research for High Magnetic Field Plasma Compression", Journal of Magnetism and Magnetic Materials, April 1979.

2. Barcilon, A., Book, D.L., and Cooper, A.L., Phys. Fluids 17, 1707 (1974).

3. Turchi, P.J., et al, Phys. Rev. Lett. 36, 1546, (1976).

4. Turchi, P.J., et al, NRL Memo Report 3536, June 1977.

5. Turchi, P.J., et al, NRL Memo Report 3511, June 1977.

6. Burton, R.L., et al, in Proc. of 7th Symposium on Engineering Problems of Fusion Research, 1977 (IEEE Pub. No. 77CH1267-4-NPS), p. 225.

7. Book, D.L. and Turchi, P.J., Comments Plasma Phys. Cont. Fusion, 4, 101 (1978).

8. Turchi, P.J., Burton, R.L., and Book, D.L. "Optimization of Stabilized Imploding Liner Fusion Reactors", in Proc. of 10th Symposium on Fusion Technology, 4-8 Sept 1978, Padova, Italy. Also in NRL Memo Report 4029.

9. Baumeister, T. and Marks, L.S., eds ., Standard Handbook for Mechanical Engineers, 7th Edition, McGraw-Hill, N.Y., Section 3-65.

10. Center for Electromechanics, Univ. of Texas, Austin, "Engineering Analysis for LINUS Imploding Liquid Liner Systems", Final Report on NRL Contract No. N00173-78-C-0084, November 1978.

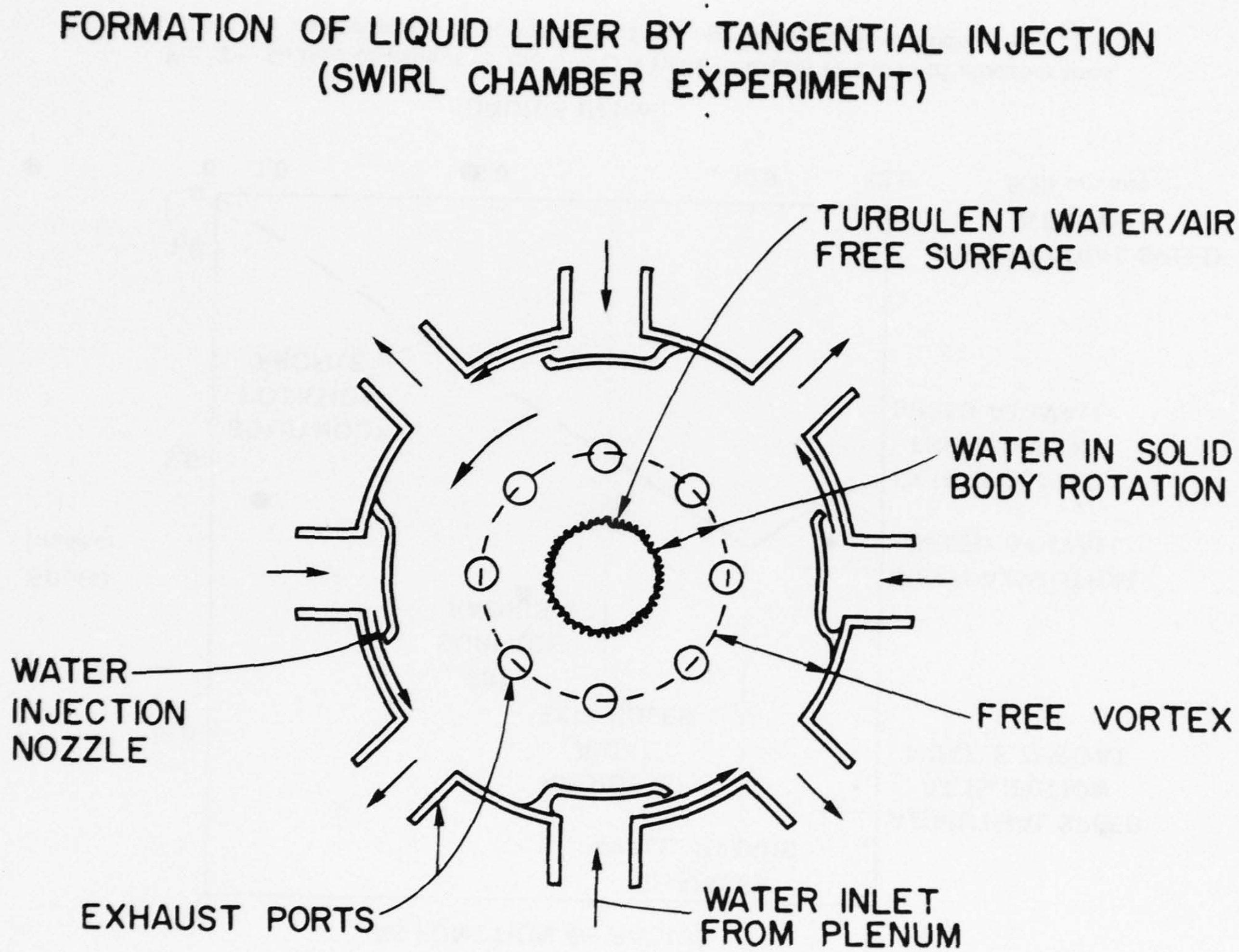

Fig. 1 — Schematic of tangential fluid injection apparatus (swirl chamber) showing positions of injection nozzles, exit ports, and the liner free-surface

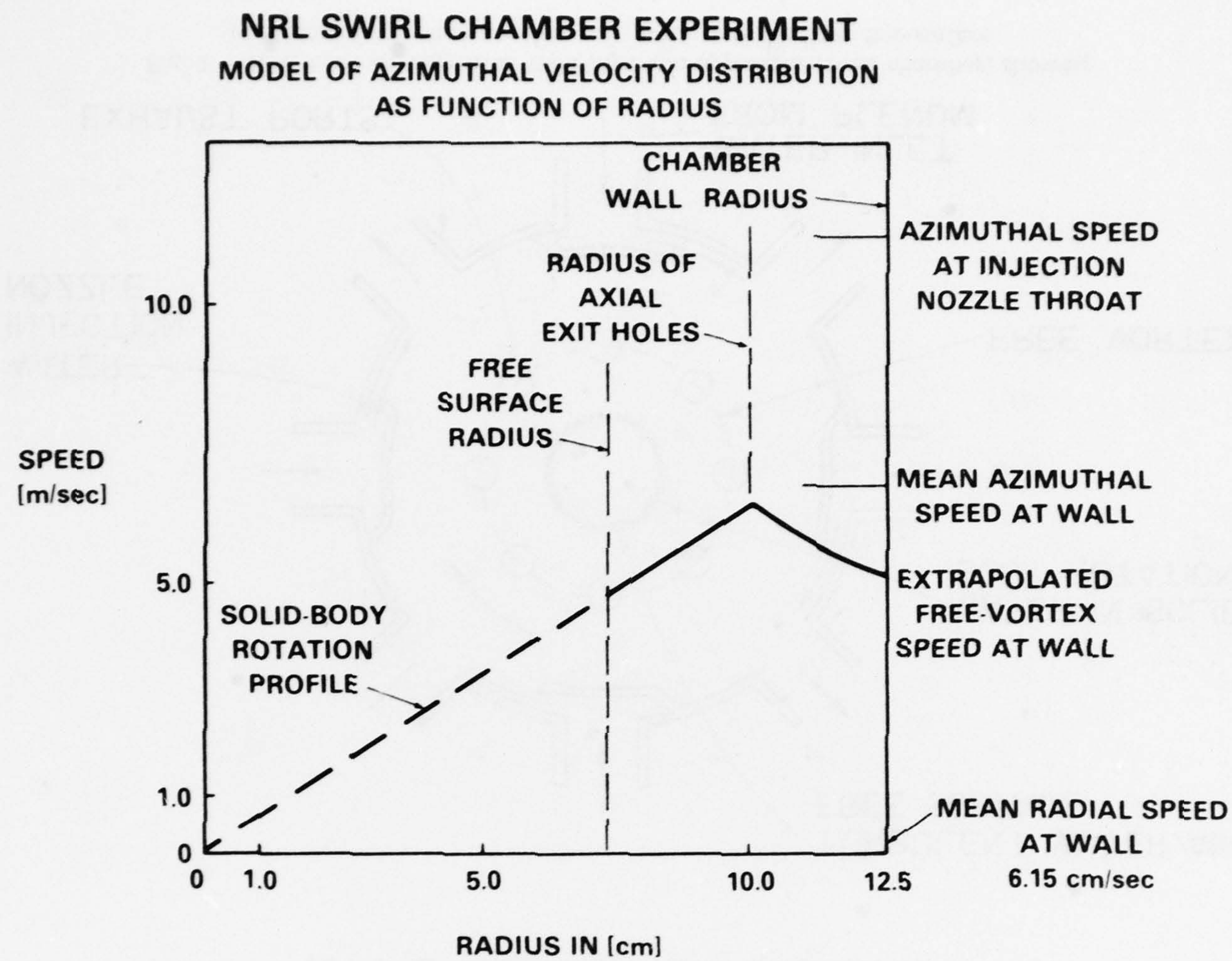

Fig. 2 — Graphs of azimuthal speed versus radial position in the swirl chamber used in derivation of power losses from open-channel flow model